

Revisiting the Ceara Rise, equatorial Atlantic Ocean: isotope stratigraphy of ODP Leg 154 from 0 to 5 Ma

R. H. Wilkens¹, T. Westerhold², A. J. Drury², M. Lyle³, T. Gorgas⁴, and J. Tian⁵

¹Hawaii Institute of Geophysics & Planetology, University of Hawaii, Honolulu, HI, 96822, U.S.A.

²MARUM, University of Bremen, Bremen, 28359, Germany

³CEOAS, Oregon State University, Corvallis, OR, 97331, U.S.A.

⁴GFZ German Research Centre for Geosciences, 14473 Potsdam, Germany

⁵State Key Laboratory of Marine Geology, Tongji University, Shanghai, 200092, China

Correspondence to: Roy H. Wilkens (rwilkens@hawaii.edu)

Abstract

Isotope stratigraphy has become the method of choice for investigating both past ocean temperatures and global ice volume. Lisiecki and Raymo (2005) published a stacked record of 57 globally distributed benthic $\delta^{18}\text{O}$ records versus age (LR04 stack). In this study LR04 is compared to high resolution records collected at all of the sites drilled during ODP Leg 154 on the Ceara Rise, in the western equatorial Atlantic Ocean. Newly developed software is used to check data splices of the Ceara Rise sites and better align out-of-splice data with in-splice data. Core images recovered from core table photos are depth and age scaled and greatly assist in the data analysis. The entire splices of ODP Sites 925, 926, 927, 928 and 929 were reviewed. Most changes were minor although several were large enough to affect age models based on orbital tuning. A Ceara Rise composite record of benthic $\delta^{18}\text{O}$ is out of sync with LR04 between 1.80 and 1.90 Ma, where LR04 exhibits 2 maxima but Ceara Rise data contain only 1. The interval between 4.0 and 4.5 Ma in the Ceara Rise compilation is decidedly different from LR04, reflecting both the low amplitude of the signal over this interval and the limited amount of data available for the LR04 stack. A regional difference in benthic $\delta^{18}\text{O}$ of 0.2 ‰ relative to LR04 was found. Independent tuning of Site 926 images and physical property data to the Laskar et al. 2004 orbital solution and integration of available benthic stable isotope data from the Ceara Rise provides a new regional reference section for the equatorial Atlantic covering the last 5 million years.

26 **1. Introduction**

27 Sedimentary archives retrieved by ocean drilling since 1968 by the Deep Sea Drilling Program (DSDP,
28 1968-1983), the Ocean Drilling Program (ODP, 1983-2003), the Integrated Ocean Drilling Program (IODP, 2003-
29 2013) and the International Ocean Discovery Program (IODP, since 2013) provide key records needed to better
30 understand processes and interactions of the Earth system. Over almost 5 decades of coring, ocean drilling samples
31 and data have contributed significantly to major breakthroughs in our understanding of earth history - including such
32 basic tenets as seafloor spreading, a detailed history of reversals of the Earth's magnetic field, evolution/extinction
33 of marine species and many more. Included in this list is the advancement of stable isotope stratigraphy and the
34 recognition of the critical part played by variations in the Earth's orbital parameters in climate history. Sites drilled
35 during ODP Leg 154 on the Ceara Rise have played a significant role in creating age models for the Neogene based
36 on astrochronology.

37 Stable isotope stratigraphy has become the method of choice for investigating both past ocean temperatures
38 and global ice volume. When global ice volumes are large, such as times of vast continental ice sheets, the world
39 oceans become enriched in ^{18}O , a "heavy" isotope of the more abundant ^{16}O . It has been demonstrated (e.g. Hays et
40 al, 1976) that variations in ^{18}O enrichment ($\delta^{18}\text{O}$) coincide with periodicities of the orbital parameters of
41 eccentricity, obliquity, and precession and their influence on the distribution and intensity of solar insolation on the
42 Earth's surface. Therefore, with a knowledge of the previous behavior of the orbital parameters (e.g. Laskar et al.,
43 2011) isotope stages (cycles) may be assigned ages to a very high degree of precision (astronomical tuning). Lisiecki
44 and Raymo (2005) published a compilation of globally distributed benthic $\delta^{18}\text{O}$ records versus age from 57 sites
45 worldwide that included data from the past 5.3 Ma (LR04 stack). Their work established a framework against which
46 almost all subsequent isotopic studies of late Neogene sediments have been compared.

47 The LR04 stack is a significant contribution for having demonstrated the global semi-synchrony of the
48 overall behavior of the $\delta^{18}\text{O}$ record in deep sea benthic stable isotope data. It does, however, have some drawbacks.
49 LR04 is an amalgam of data with various resolutions from sites in different oceans and different latitudes, thus
50 averaging regional signals into the overall stack. The age models used for the individual data sets depend on
51 chronological markers such as the ages of magnetic field reversals that may have changed since the original studies
52 were completed and new data has been reported. Astronomical tuning is complicated by the dominance of obliquity
53 in records from sediments older than 1.2 Ma because the pattern of consecutive cycles are similar. And finally,
54 almost all of the $\delta^{18}\text{O}$ profiles were derived from spliced data. Splicing is a technique used at drilling sites to piece
55 together one continuous record from adjacent drill holes (Ruddiman et al, 1987; Hagelberg et al., 1992). Splices may
56 be subject to cycle skipping or duplication of events when data are aligned from different holes. Averaging of
57 multiple sites will compensate for small errors in the spliced records if many sites are used and most have a correct
58 splice. As with age models, splices may evolve over time as more detailed and new types of data are gathered post-
59 cruise and reveal previously missed or doubled $\delta^{18}\text{O}$ patterns (see Westerhold et al. 2014, supplementary Fig. S9).

60 There are 21 records included in LR04 that extend to ages older than 3 Ma included in LR04, and only 14
61 that have data older than 4 Ma. As the numbers in the stack shrink, the importance of having well-spliced records
62 grows. A number of records used in LR04 contain problematic succession with respect to their composite record.

63 Site 982, for example, is one of the high-resolution sites that extends beyond 3 Ma (Venz et al. 1999, Venz and
64 Hodell 2002), and has been used subsequently to transfer age models to other isotope records (Drury et al. 2016).
65 However, there is controversy over the composite record of 982 as well as the age model (Lawrence et al. 2013,
66 Khelifi et al. 2012, Bickert et al. 2004).

67 For the interval 1.7-5.3 Ma the LR04 stack depends heavily on the spliced records from Leg 138 - the S95
68 benthic composite stack (Shackleton et al., 1995). It was noted in Lisiecki and Raymo (2005) that for marine isotope
69 stages (MIS) M2 and MG2 at 3.35 Ma there is a mismatch of data and a potential coring or splicing problem in Site
70 846. Even so, Site 846 was used for the initial alignment in LR04 from 2.7-5.3 Ma along with Site 849 (1.7 - 3.6
71 Ma) and Site 999 (3.3 - 5.3 Ma). Any problem in the spliced records of the sites used for initial alignment will
72 propagate through the stack if not compensated by a large number of additional sites. Thus we might expect a
73 greater possibility of erroneous correlation in older less repeated parts of the stack, particularly where the amplitude
74 of the $\delta^{18}\text{O}$ variations are relatively small (see Lisiecki and Raymo 2005 - Fig. 2).

75 In order to provide a precise age model the LR04 stack was tuned to a non linear ice volume model forced
76 by insolation (65°N) using the Laskar et al. (1993) 1,1 orbital solution including an assumed decrease in the lag of
77 ice sheet response to insolation forcing. To test and evaluate the LR04 stack and the tuning approach from 0 - 5 Ma,
78 a robust composite record from a single location combined with an astronomical age model that is independent of
79 ice volume modeling is required. Furthermore, extending the $\delta^{18}\text{O}$ stack into the Miocene means that robust
80 composite records are required to avoid misalignments and tuning errors at the outset. Sediments from the Ceara
81 Rise (South Atlantic) are perfectly suited for testing because they contain orbitally driven changes and are already
82 the backbone for astronomical calibration of the Geological Time Scale for the last 14 Ma (Shackleton and
83 Crowhurst 1997, Zeeden et al. 2013, 2014, Lourens et al. 2004).

84 Here we revisit data collected during, and subsequent to, ODP Leg 154 (Fig. 1). The LR04 stack includes
85 benthic stable isotope data from ODP Leg 154 Sites 925, 927, 928, and 929. Site 927 was used for initial alignment
86 from 0–1.4 Ma in LR04. Site 926 is also considered a primary site for time scale constructions for 0-15 Ma and is
87 independent of LR04. In this study, we use newly developed software to check and improve the composite records
88 of Leg 154. We then stretch and squeeze data outside the splice, use core images to correlate all sites to the Site 926
89 depth scale, orbitally tune the core images, and compare the age model with the LR04 stack for the past 5 Ma. The
90 new software system greatly facilitates the construction of benthic $\delta^{18}\text{O}$ reference records back into the Miocene
91 from single regions. Regional astronomically tuned $\delta^{18}\text{O}$ records are a next important step in deciphering
92 paleoceanographic conditions worldwide.

93

94 **2. Material and Methods**

95 The proliferation and diversity of the data collected both during and after ocean drilling cruises can at times
96 be somewhat overwhelming for the individual scientist. Data are now freely available through online data bases
97 maintained by the ocean drilling infrastructure for cruise results (e.g. [LIMS](#), [JANUS](#)), by national efforts (e.g.
98 [NGDC](#)) or community efforts (e.g. [PANGAEA](#)). However, a unified and consistent system for integrating disparate
99 data streams such as micropaleontology, physical properties, core images, geochemistry, and borehole logging has

100 not been widely available. In this section we describe a system that we have developed over several years to work
101 with ocean drilling data and images (CODD - Code for Ocean Drilling Data). CODD takes advantage of the
102 versatile graphical user interface and analytical functions contained in the [IGOR™](#) graphing and analysis program
103 commercially available from Wavemetrics, Inc. One of the great advantages of a modern analysis program like
104 IGOR™ paired with new computers and fast processors is the ability to use images as data. Rather than a static
105 picture of a core or section, images are scaled and plotted along with traditional data versus depth or age. Core
106 images may be squeezed, stretched, subsampled, and concatenated, allowing for great versatility. The CODD set of
107 ocean drilling macros for IGOR™ and a User Guide are freely available at www.CODD-Home.net. Core images,
108 both as png files and scaled IGOR binaries as well as all tables of this study including age models, offsets, splices,
109 tie points between sites, spliced MS data, isotope data, and mapping pairs for squeezing and stretching of cores are
110 available through the open access Pangaea website under <https://doi.pangaea.de/10.1594/PANGAEA.870873>.

111

112 **2.1 Data Structure**

113 The heart of the CODD data structure is the coring matrix - a 3 layered array in which the top layer
114 contains the original depth to the top of each section (mbsf - meters below seafloor) sorted by core (rows) and
115 sections (columns). The middle layer contains the length of the sections and the third layer the composite depth
116 (mcd - meters composite depth). Sample depths are calculated by referencing the proper layer and coordinate by
117 core and section and then adding the sample interval. The reverse process of returning the core, section, and interval
118 designation of a given sample depth is accommodated by comparing it to the section top depth plus the section
119 length to find where the sample originated.

120 A standardized naming convention is essential to efficient processing of multiple and diverse data streams.
121 In CODD data are assigned 3 part names, Hole, Technique and Information, separated by underscores. Thus
122 gamma-ray attenuation depths are U925A_GRA_MBSF and U925A_GRA_MCD with data as U925A_GRA_GRA.
123 Core, section, interval and age are similarly named. Isotope data might be U925A_Iso_d18O and U925A_Iso_d13C.
124 While the Hole and Technique designations must be identical for a single data set, the Information may be anything
125 the user desires, including new data like ratios created from existing information. IGOR™ records data processing
126 steps and the use of a standard naming convention allows users to repeat processing for different data by simply
127 replacing one Hole or Technique with another in the recorded steps. It also simplifies the development of
128 automation macros. This is essential for processing large amounts of data from multiple drill-holes and drill-sites -
129 especially when changes to composite records (splices) are needed.

130

131 **2.2 Image Processing**

132 Ever since IODP Leg 200, core section images have been captured by line scanners as discrete files which
133 are easily loaded into analysis programs with little or no preparation. However, the only access to core images from
134 the first approximately 200 ocean drilling cruises are through digitized photographs of entire cores laid out on a
135 table in parallel sections (Fig. 2A). CODD includes a module for cutting core section images from core table photo
136 images, correcting them for uneven lighting, scaling them to mbsf (meters below seafloor) and combining them into

137 a single core image (Fig. 2B) through a series of simple steps. In general, the outer 5% of each section image is
138 excluded to minimize friction effects of coring that tend to bend horizontal layers. In practice it takes between 1 and
139 2 minutes to go from loading a core table photo to producing a scaled composite core image. The visualization and
140 impact of the scaled composite is very much different from the core table photo and of much greater value during
141 data analysis. The use of scaled composite core images has proven to be particularly effective in creating site splices
142 or for the checking of existing splices.

143 Lighting correction is a necessary step when using images cut from core table photos because the light
144 source used for the original photos was co-located with the camera above the center of the core table, resulting in the
145 center of the picture being brighter than the edges (Schaaf and Thurow, 1994; Nederbragt and Thurow, 2001, 2005).
146 This effect is illustrated by profiles of lightness from H S L (hue, saturation, lightness) representations of section
147 images plotted together (Fig. 2A inset). For these sections the variability of the intensity of lightness, excepting
148 some spikes representing darker layers, is around 50 units of lightness (out of a full scale of 0 - 255). The difference
149 from the center to the ends of the best-fit line to the profiles is approximately 25 lightness units, so uneven lighting
150 has a significant effect on the section images. When the core table photos are viewed, the observer's eyes and mind
151 make a correction and the uneven lighting seems subtle, but we have found that when stringing section images
152 together to make a composite core image the 1.5 m long lighter/darker cycles are readily apparent. As many ocean
153 drilling sediment cores vary in lightness as a function of carbonate and/or biogenic silica content (e.g. Balsam et al.,
154 1999), lighting cycles in core images degrade the usefulness of core color or lightness profiles as proxies for other
155 properties of interest or for spectral analysis. Thus CODD processing of core table photos includes a step which fits
156 a line to the lightness profiles and then applies a "flattening" filter which brightens the section images away from the
157 center according to the fit. While not perfect, the process removes most of the 1.5 m color cyclicity (Fig. 2B). There
158 is also lighting variation across the core box images that can produce a 9/10 m cycle in the spliced composite
159 images. It appears to be somewhat more diffuse than the along-core section variation and hasn't hindered the present
160 work. We are developing a process to correct for lighting variation of the entire core box image prior to cutting the
161 individual section images. This may also allow us to remove the color cast present in many of the older core box
162 images, such as the purplish hue seen in Fig. 2A.

163

164 **2.3 Splicing, Stretching, and Squeezing**

165 In the same manner that sections may be strung together to make a composite core image, extracted splice
166 sections of core images from different holes can be merged into a single scaled spliced site image (Fig. 3a). Splicing
167 is a 2 step process, the first of which involves offsetting the mbsf depth for individual cores to a composite depth by
168 aligning features in data collected from multiple holes. It is worth noting here that it is rare that all features in
169 individual cores from different holes align - as coring disturbance (e.g. extension or compression at the top and
170 bottom of piston cores, see Ruddiman et al, 1987 for an in depth discussion) or natural variability mean that while
171 one feature may align, another is offset (e.g. Lisiecki and Herbert, 2007). The individual setting the splice (the
172 correlator) makes a decision as to which feature to align based on overall considerations of the splicing process.
173 Once the core offsets are set, the correlator chooses tie points between holes to produce as complete a sedimentary

174 record as possible while avoiding any possible duplication. In the past this has been done using data profiles of
175 properties measured on whole round core sections - primarily density from Gamma Ray attenuation (GRA), and
176 magnetic susceptibility (MS) as well as reflectance spectrophotometer intensity (RSC) on split sections. This can
177 prove to be tricky when using data that are replete with similar cycles. Cycle skipping or doubling is a constant
178 source of potential error and the inclusion of images in the process helps greatly. While checking splices or splicing
179 cores and choosing tie points we used the same criteria as typically used by the shipboard stratigraphic correlator for
180 (I)ODP expeditions. The splice should contain no coring gaps and disturbed sections are avoided. Where possible
181 we avoided using the top and bottom ~0.5 m of cores, where disturbance resulting from drilling artifacts is most
182 likely. Those portions of the recovered core most representative of the overall stratigraphic section of the site are
183 picked and the number of tie points is minimized to simplify sampling.

184 An example from Ceara Rise Site 927 demonstrates image utility while examining an existing splice. A 10
185 m long section of images and data is presented in Fig. 3. Poor agreement between offset data from all three holes of
186 Site 927 occurs around 50 mcd, immediately below a splice tie in the published splice for the site (Fig. 3A). The
187 images show poor agreement between the light and dark bands in cores 927C-05H and 927B-06H. A better solution
188 is obtained by reducing the offset of 927B-06H by 1.6 m to align the peak in RSC seen around 50.2 mcd in 927C-
189 05H with a similar peak at 51.8 mcd in 927B-06H (Fig. 3B, 3C). Fortunately, because the core images are depth
190 scaled, CODD allows us to shift and re-splice both core images and all other datasets using a simple algorithm. The
191 resultant shift shows better agreement between images and data from both holes. Significantly, the shift illustrated
192 removes one 40 ka obliquity cycle from the isotope record (Bickert et al. 1997) and will alter a tuned age model
193 accordingly.

194 Traditionally, once the splice has been set, subsequent samples are taken and measurements made only
195 from the core material included in the splice. While three or more holes are often cored at sites devoted to
196 paleoceanographic studies, the volume of samples available within a splice is equivalent to a single hole. And since
197 archival halves of each core are reserved for later sampling, it is often difficult to obtain new samples along a
198 heavily sampled section of the splice. More material is available from sections of cores not included in the splice,
199 but as mentioned above, the process of aligning and offsetting cores from adjacent holes by matching features is
200 imperfect due to coring effects and natural variability (e.g. Lisiecki and Herbert 2007, Wilkens et al, 2009).
201 Misalignment of off-splice features may add significant noise when in-splice and out-of-splice data are combined. In
202 order to align features from sections of core not included in the splice it is necessary to stretch/squeeze images and
203 data outside the splice. Magnetic susceptibility data have been stretched from the off-splice data to the splice in Fig.
204 4. Using CODD, sets of tie points between off-splice data and the splice for each hole (yellow numbers in Fig. 4) are
205 selected using cursors. Stretched data and images are updated in real time. The tie points allow investigators to
206 interpolate out-of-splice mcd depths to their equivalent levels in the splice.

207 The ability to squeeze and stretch data and images has a second useful application. Sites drilled in the same
208 general area of the ocean, such as those on the Ceara Rise, often share many physical features in data such as
209 density, magnetic susceptibility, or color in their sediment columns. In a manner similar to the process of stretching
210 and squeezing off-splice data to the splice, CODD employs a cursor driven routine to stretch data and images from

211 different sites to a single common depth scale using similar features. The segment of the stretch of Site 927 to Site
212 926 between tie points 60 and 80 is illustrated in Fig. 5. In total, 428 pairs of tie points were identified while
213 matching the upper 304 mcd of Site 927 to the upper 285 mcd of Site 926. Additional constraints such as
214 paleomagnetic reversals and biostratigraphic events may be included, helping to guide the correlation. In practice a
215 user views multiple data types and images simultaneously and tie points selected from one data set are mapped to all
216 others at the same time.

217

218 **2.4 Depth to Age**

219 Once data and images from the individual sites have been tied to a common depth scale the final CODD
220 processing step is to set everything to a single age model. We used the age models of Bickert et al (1997) and
221 Tiedemann and Franz (1997), adjusted for our splice corrections and updated to Laskar et al. (2004), to compare
222 age-scaled images and data from the various Ceara Rise sites. An example comparing Sites 926 and 927 is presented
223 in Fig. 6. Comparison of the composite images is remarkable for the fact that individual sedimentary layers that
224 represent sometimes less than 10 kyr are readily identifiable between sites. This suggests that in areas where the
225 sediment has enough color variation highly targeted samples may be collected that represent precisely the same
226 event at multiple sites.

227 MS data and the composite image of Site 926 are compared with orbital calculations using Laskar et al.
228 (2004) in Fig. 7. The orbital curve was calculated using 100% of the eccentricity (E) effect plus 50% of the obliquity
229 (T) and precession (P) intensities. Correlation of the MS data to the Laskar model was the primary basis for the
230 Bickert et al. (1997) and Tiedemann and Franz (1997) age models, so agreement between the 2 curves is expected.
231 [They used a correspondence between MS maxima and northern hemisphere summer insolation minima to develop](#)
232 [their age models. This phase relationship was found to be most consistent in both precession and obliquity frequency](#)
233 [bands \(Shackleton and Crowhurst 1997\). See Zeeden et al., 2013 for a concise description of their approach.](#)
234 Comparison with a composite core image was not possible for those earlier investigators and our results illustrate the
235 remarkably detailed agreement between cycles seen in the calculations and variations in sediment color. Based on
236 these observations and the well-known phase relationship (Bickert et al. 1997) we refined the tuning for Site 926
237 tying dark (light) layers, which correspond to MS maxima, to ET-P minima (maxima). We used only the core image
238 and color reflectance for tuning; therefore plotting the magnetic susceptibility data versus insolation serves as a
239 crosscheck for a consistent phase relationship throughout the record.

240

241 **3. Results**

242 We checked the entire splices of Sites 925, 926, 927, 928 and 929 for the last 5 Ma. Most of the changes in
243 the published splice tables were minor although several, such as the one illustrated in Fig. 3, were large enough to
244 affect age models based on orbital tuning. Data from samples outside of the revised splices were aligned with the
245 splice based on stretching and squeezing of the out-of-splice data. Mapping pairs to convert depths outside of the
246 splice to the composite depth are provided in supplemental files. For the interval spanning 0 to 5 Ma we compiled
247 5533 benthic $\delta^{18}\text{O}$ isotope measurements from Bickert et al. (1997), deMenocal et al. (1997), Tiedemann and Franz

248 (1997), Shackleton and Hall (1997), Billups et al (1998) and Tiedemann and Franz (1997). Data were plotted on the
249 updated age model for Site 926. Data from all of the sites are compared with one another and a smoothed curve
250 (Gaussian filter) combining all of the sites is compared to LR04 in Fig. 8. Data tables for core offsets, splices, and
251 age models are available as supplemental files to this publication.

252 Agreement amongst the different Ceara Rise Sites is good in terms of the shapes of the curves while there
253 is a spread in absolute values. This is likely due to the water depths at the different sites, which ranged from 3040 m
254 at Site 925 to 4355 m at Site 929. Offsets in benthic oxygen isotope data between Site 925 and Site 929 in some
255 intervals (e.g. 3.6 to 4.5 Ma) have been suggested to indicate a relatively warmer and saltier NADW than today
256 (Billups et al. 1997).

257 The overall agreement between the Ceara Rise smoothed composite oxygen isotope curve and the LR04
258 global compilation is generally quite good although there is a definite difference in absolute values with the Ceara
259 Rise data exhibiting consistently lower values of about 0.2 ‰ than LR04 (Supplementary Fig. S1). The 0.2 ‰ offset
260 is well within the potential regional differences of up to 0.3 ‰ cited by Lisiecki and Raymo (2005). The consistency
261 of the difference over the entire 5 Myr scope of this study is remarkable given the regional mix of data used for
262 LR04.

263 While the agreement between Ceara Rise and LR04 oxygen isotope data is good, there are discrepancies in
264 some intervals. The 2 curves are out of sync between 1.80 and 1.90 Ma with LR04 exhibiting 2 maxima whereas
265 Ceara Rise contains only 1. As this is close to a point where the LR04 stack switched from Site 677 (0-2 Ma) and
266 Site 927 (0-1.7 Ma) to Site 849 (1.7-3.6 Ma), misalignments in the stack between single sites with the original
267 spliced records could have led to a mismatch here. Tuning for Site 926 in this interval is robust and does not allow a
268 shift that could accommodate the mismatch. Hence the interval from 1.80 and 1.90 Ma in the LR04 stack has to be
269 revised. Even larger differences are seen between 4.0 and 4.5 Ma (Fig. 9). Data from Site 929 have been shifted
270 +0.25 ‰ in Fig. 9 to aid in the comparison of the excursions in the data. The data from Sites 925 and 929 are in
271 good agreement, but the Ceara Rise smoothed compilation, which is almost entirely composed of data from the 2
272 sites over this age interval, bears little resemblance to LR04. As pointed out in Lisiecki and Raymo (2005), their
273 stack prior to 4 Ma includes far fewer sites than the more recent data. The 4.0 to 4.5 Ma interval is also one of low
274 amplitude variability in $\delta^{18}\text{O}$ as a response to orbital variation, making the tuning effort at the individual sites
275 contributing to LR04 more difficult than at later time intervals. Better correlation of data older than 4.5 Ma suggests
276 that age model uncertainties are confined to 4.0 - 4.5 Ma and do not necessarily offset the age models for older
277 sediments in LR04 or our compilation.

278 Accessing uncertainty in the age model is difficult and cannot be discussed in this manuscript as it would
279 require extensive testing. However, in Zeeden et al. (2013) and (2014) this is already done with regards to the
280 uncertainty in the target curve. The outstanding match of sedimentary pattern and insolation calculations, which is
281 amazing, keeping in mind that the Laskar et al. 2004 model is based on a relatively short time of observational data,
282 gives confidence that the error for the Miocene is less than a single precession cycle. Due to the excellent match in
283 patterns we think the main error lies in the accuracy of the target (precession and obliquity). The error in precession

284 maxima and minima positions will be only relevant for times older than 5 Ma (see Lourens et al. 2004), as already
285 discussed in the Zeeden et al. (2013, 2014) papers.

286

287 **5. Discussion**

288 Independent tuning of Site 926 images and physical property data to the Laskar 2004 orbital solution and
289 integration of available benthic stable isotope data from the Ceara Rise provides a new regional reference section for
290 the equatorial Atlantic covering the last 5 million years. Comparing the CODD based new stack from the Ceara Rise
291 to the LR04 stack reveals overall very good agreement suggesting that most of the LR04 stack is robust for the
292 interval from 0-4 Ma. Disagreement in the interval from 1.8-1.9 Ma (Fig. 9) points to uncertainties in the records of
293 Sites 677 and 849. The record of Site 677 (Shackleton et al., 1990) has a gap in the composite around this time
294 interval at 85 mcd. Our unpublished re-examination of the Mix et al. (1995) Site 849 age model suggests that it
295 might be affected by issues in the composite record revolving around core 849C 5H at around 52 mcd. Construction
296 of an equatorial Pacific stack, presently underway, should resolve the issue.

297 The differences between LR04 and the Ceara Rise average between 4 and 4.5 Ma reveals a more complex
298 matter that questions assumptions made in LR04. The tuning in Site 926 (Fig. 10) in this interval is robust and can
299 not be changed. The match between the precession-dominated insolation curve and the dark/light pattern shown in
300 the composite site image is excellent. To match the LR04 and the Ceara Rise isotope stacks, the Ceara Rise stack
301 needs to be shifted by 21 kyr to older ages between 4.1 and 4.3 Ma - which is not possible without changing the
302 phase relation between insolation and the dark/light pattern of the Ceara Rise sediments. The LR04 stack is basically
303 tuned to obliquity in this interval with lighter $\delta^{18}\text{O}$ in obliquity maxima. The major discrepancy at 4.2 Ma occurs in
304 an interval of low obliquity amplitude and higher precession amplitude modulation (Fig. 11). Lighter $\delta^{18}\text{O}$ values
305 match insolation maxima in the interval around 4.2 Ma, thus suggesting that the cyclic changes in $\delta^{18}\text{O}$ are related to
306 precession rather than obliquity. Moreover, the minimum in $\delta^{18}\text{O}$ at 4.18 Ma and the maximum at 4.21 Ma in the
307 Ceara Rise stack do not correlate to obliquity minima and maxima as they do before and after this interval, which
308 coincides with a minimum in the 1.2 myr obliquity amplitude modulation. A closer look at the individual isotope
309 records at Ceara Rise (Fig. 12) reveals that these cycles are indeed precession cycles, seen in the site composite
310 image as well as in the benthic $\delta^{18}\text{O}$ data. We therefore conclude that the LR04 stack misinterpreted these two cycles
311 as one obliquity cycle that then was used to tune the LR04 age model. According to the Ceara Rise tuning this
312 interval is not related to obliquity but rather to precession variations. This means that the assumption in LR04
313 matching all cycles to obliquity is dangerous in intervals of low obliquity amplitude and can lead to incorrect tuning
314 results.

315 Further study of splices and age models used in the data contributing to LR04 will be needed before these
316 discrepancies can be fully resolved. Such clarification is a necessary step in the ongoing effort to create a global
317 correlation of isotope and other data that can be resolved at the isotopic stage level. Such examination of other areas
318 of the oceans will also aid in the development of regional isotope curves to compare with our findings for the Ceara
319 Rise. The CODD approach is a useful tool for extending oxygen isotope reference records into the Miocene and
320 beyond. Combining multiple records from several sites drilled in an oceanic region is greatly facilitated by CODD

321 and helps to form a regional stratigraphic framework. Stacked records from different regions, such as the equatorial
322 Pacific, are urgently needed to test and verify the completeness of each record as gaps can occur on a regional scale.
323 Establishing high resolution age models on a regional scale is key to understanding paleoceanographic changes on
324 orbital timescales for the entire Cenozoic.

325

326 **6. Conclusions**

327 We have demonstrated a new system for capturing core images as data using newly developed CODD
328 software. The ability to transform core table photos and line-scans of core sections into data as depth or age scaled
329 core images has helped greatly in the task of revising published splices for Ceara Rise sediments cored during ODP
330 Leg 154. Comparison of the revised data with the LR04 global oxygen isotope stack reveals that there are sections
331 of the stack that are not well resolved. Further study of data contributing to LR04 will lead to a clarification of the
332 misfits we have found as well as establishing other regional isotope offsets from a global stack. The CODD software
333 package thus can play a key role in the construction of a new generation of the benthic isotope stack and surely will
334 be very helpful in extending the stack into the Miocene. The next important step will be to form a more robust and
335 accurately tuned initial signal used to form the benthic isotope stack.

336

337 **Acknowledgements**

338 Development of CODD was partially supported by post cruise funds from U.S. Science Support for RW.
339 Financial support for this research was also provided by the Deutsche Forschungsgemeinschaft (DFG) to TW and
340 AJD.

341

342

343 **References**

344 Bickert, T., Curry, W. B. and Wefer G.: Late Pliocene to Holocene (2.6– 0 Ma) western equatorial Atlantic deep-
345 water circulation: Inferences from benthic stable isotopes, *Proc. Ocean Drill. Program Sci. Results*, 154, 239–
346 254.1997.

347
348 Bickert, T., G. H. Haug, and R. Tiedemann: Late Neogene benthic stable isotope record of Ocean Drilling Program
349 Site 999: Implications for Caribbean paleoceanography, organic carbon burial, and the Messinian Salinity Crisis,
350 *Paleoceanography*, 19, PA1023, doi:10.1029/2002PA000799, 2004.

351
352 Billups, K., Ravelo, A.C. and Zachos, J. C.: Early Pliocene deep water circulation in the western equatorial Atlantic:
353 Implications for high-latitude climate change, *Paleoceanography*, 13, 84–95,1998.

354
355 deMenocal, P., Archer, D. and P. Leth: Pleistocene variations in deep Atlantic circulation and calcite burial between
356 1.2 and 0.6 Ma: a combined data-model approach, in Shackleton, N.J., Curry, W.B., Richter, C., and Bralower, T.J.
357 (Eds.), *Proc. of the Ocean Drilling Program, Scientific Results*, Vol. 154, 285-298,
358 doi:10.2973/odp.proc.sr.154.113.1997.

359
360 Drury, A.J., Westerhold, T., Frederichs, T., Wilkens, R., Channell, J., Evans, H., John, C., Lyle, M., and Tian, J.:
361 Late Miocene time scale reconciliation: accurate orbital calibration from a deep-sea perspective, *Paleoceanography*,
362 in press, 2016.

363
364 Hagelberg, T, Shackleton, N., Pisias, N., and Shipboard Scientific Party,: Development of composite depth sections
365 for Sites 844 through 854, In Mayer, L., Pisias, N., Janecek, T, et al., *Proc. ODP, Init. Repts.*, 138 (Pt.1): College
366 Station, TX (Ocean Drilling Program), 79 85, doi:10.2973/odp.proc.ir.138.105.1992.

367
368 Hays, J.D., Imbrie, J. and Shackleton, N.J.: Variations in the Earth's orbit: Pacemaker of the ice ages., *Science*, 194,
369 1121-1132, doi:10.1126/science.194.4270.1121, 1976.

370
371 Khélifi, N., Sarnthein, M., and Naafs, B. D. A.: Technical note: Late Pliocene age control and composite depths at
372 ODP Site 982, revisited: *Clim. Past*, v. 8, p. 79-87, 2012.

373
374 Laskar, J., Robutel, P., Joutel, F., Gastineau, M., Correia, A., and Levrard, B.: A long-term numerical solution for
375 the insolation quantities of the Earth, *Astron. Astrophys.*: 428, 261–285, doi:10.1051/0004-6361:20041335, 2004.

376
377 Laskar, J., Fiengo, A., Gastineau, M., and Manche H.: La2010: a new orbital solution for the long-term motion of
378 the Earth, *Astron & Astrophys*, 532, A89, pp. 15, doi:10.1051/0004-6361/201116836, 2011.

379

380 Lawrence, K. T., Bailey, I., and Raymo, M. E.: Re-evaluation of the age model for North Atlantic Ocean Site 982
381 and arguments for a return to the original chronology: *Clim. Past*, v. 9, no. 5, p. 2391-2397, 2013.
382

383 Lisiecki, L. and Raymo, M.: A Pliocene-Pleistocene stack of 57 globally distributed benthic $\delta^{18}\text{O}$ records,
384 *Paleoceanography*, 20, PA1003, doi:10.1029/2004PA001071, 2005.
385

386 Lourens, L., Hilgen, F., Shackleton, N., Laskar, J. and Wilson D.: The Neogene Period, in *A Geologic Time Scale*,
387 edited by F. Gradstein, J. Ogg, and A. Smith, pp. 409–440, Cambridge Univ. Press, Cambridge, 2004.
388

389 Mix, A. C., Pisias, N. G., Rugh, W., Wilson, J., Morey, A. and Hagelberg T. K.: Benthic foraminifer stable isotope
390 record from Site 849 (0–5 Ma): Local and global climate changes, *Proc. Ocean Drill. Program Sci. Results*, 138,
391 371–412, 1995.
392

393 Nederbragt, A.J., Thurow, J.W., 2005. Digital sediment colour analysis as a method to obtain high resolution climate
394 proxy records, in: Francus, P. (Ed.), *Image Analysis, Sediments and Paleoenvironments, Developments in*
395 *Paleoenvironmental Research*. Springer Netherlands, pp. 105–124.
396

397 Nederbragt, A.J., Thurow, J.W., 2001. A 6000 yr varve record of Holocene climate in Saanich Inlet, British
398 Columbia, from digital sediment colour analysis of ODP Leg 169S cores. *Mar. Geol.* 174, 95–110.
399 doi:10.1016/S0025-3227(00)00144-4
400

401 Ruddiman, W.F., Cameron, D., Clement, B.M., 1987. Sediment disturbance and correlation of offset holes drilled
402 with the hydraulic piston corer - Leg 94. *Initial Rep. Deep Sea Drill. Proj.* 94, 615–634.
403

404 Shackleton, N. J., Berger, A. and Peltier W. R.: An alternative astronomical calibration of the Lower Pleistocene
405 timescale based on ODP Site 677, *Trans. R. Soc. Edinburgh Earth Sci.*, 81, 251–261, 1990.
406

407 Shackleton, N.J., Crowhurst, S.J.: Sediment fluxes based on an orbitally tuned time scale 5 Ma to 14 Ma, Site 926.
408 In: Curry, W.B., Shackleton, N.J., Richter, C., Bralower, T. (Eds.), *Proceedings of the ODP, Scientific Results*, vol.
409 154. Ocean Drilling Program, College Station, TX, pp. 69–82, 1997.
410

411 Shackleton, N. and Hall, M.: The late Miocene isotope record, Site 926, in Shackleton, N.J., Curry, W.B., Richter,
412 C., and Bralower, T.J. (Eds.), *Proc. of the Ocean Drilling Program, Scientific Results*, Vol. 154, 1997.
413

414 Tiedemann, R., and Franz, S. O.: Deepwater circulation, chemistry, and terrigenous sediment supply in the
415 equatorial Atlantic during the Pliocene, 3.3–2.6 Ma and 5–4.5 Ma, *Proc. Ocean Drill. Program Sci. Results*, 154,
416 299–318, 1997.

417
418 Venz, K. A., and Hodell, D. A.: New evidence for changes in Plio-Pleistocene deep water circulation from Southern
419 Ocean ODP Leg 177 Site 1090, *Palaeogeogr. Palaeoclimatol. Palaeoecol.*, 182, 197– 220, doi:10.1016/S0031-
420 0182(01)00496-5, 2002.

421
422 Venz, K.A., Hodell, D.A., Stanton, C., and Warnke, D.A.: A 1.0 Myr record of glacial North Atlantic Intermediate
423 Water variability from ODP Site 982 in the Northeast Atlantic. *Paleoceanography*, 14, 42–52,
424 doi:10.1029/1998PA900013, 1999.

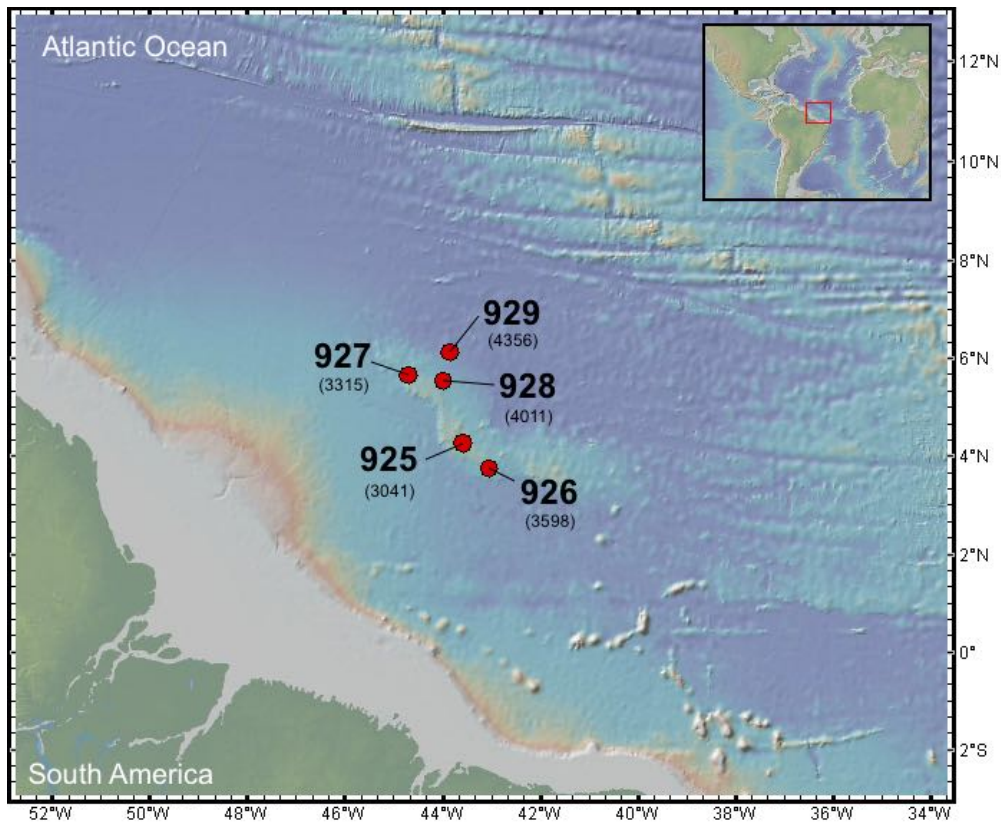
425
426 Westerhold, T., Röhl, U., Pälike, H., Wilkens, R., Wilson, P.A., and Acton, G.: Orbitally tuned timescale and
427 astronomical forcing in the middle Eocene to early Oligocene, *Clim. Past.*, 10, 955-973, doi:10.5194/cp-10-955-
428 2014, 2014.

429
430 Wilkens, R.H., Niklis, N., and Frazer, M.: Data report: digital core images as data: an example from IODP
431 Expedition 303. *In* Channell, J.E.T., Kanamatsu, T., Sato, T., Stein, R., Alvarez Zarikian, C.A., Malone, M.J., and
432 the Expedition 303/306 Scientists, *Proc. IODP*, 303/306: College Station, TX (Integrated Ocean Drilling Program
433 Management International, Inc.). doi:10.2204/iodp.proc.303306.201.2009.

434
435 Zeeden, C., Hilgen, F. J., Westerhold, T., Lourens, L., Röhl, U., and Bickert, T.: Revised Miocene splice,
436 astronomical tuning and calcareous plankton biochronology of ODP Site 926 between 5 and 14.4 Ma,
437 *Paleogeography, Paleoclimatology, Palaeoecology*, 369, 430-451, dx.doi.org/10.1016/j.palaeo.2012.11.009, 2013.

438
439 Zeeden, C., Hilgen, F. J., Hüsing, S. K., and Lourens, L. L.: The Miocene astronomical time scale 9–12 Ma: New
440 constraints on tidal dissipation and their implications for paleoclimatic investigations, *Paleoceanography*, 29,
441 2014PA002615, 10.1002/2014PA002615, 2014201

442

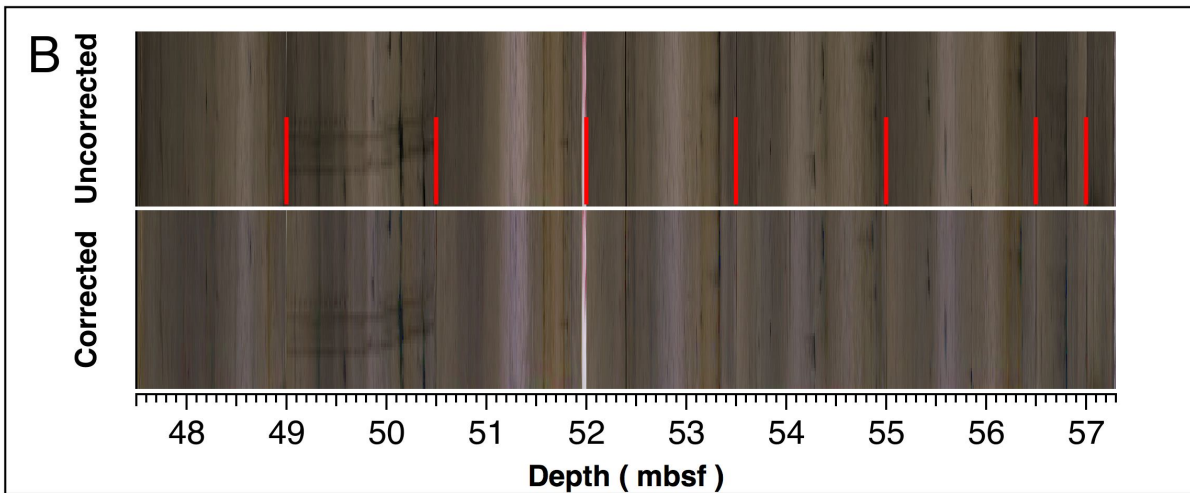
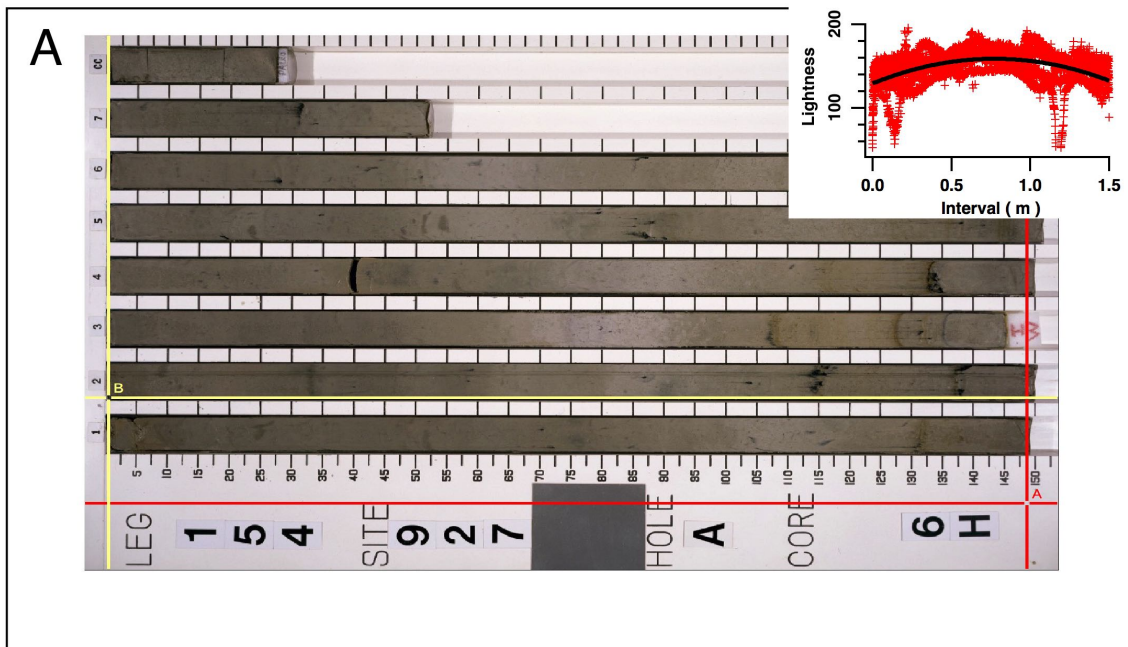


443

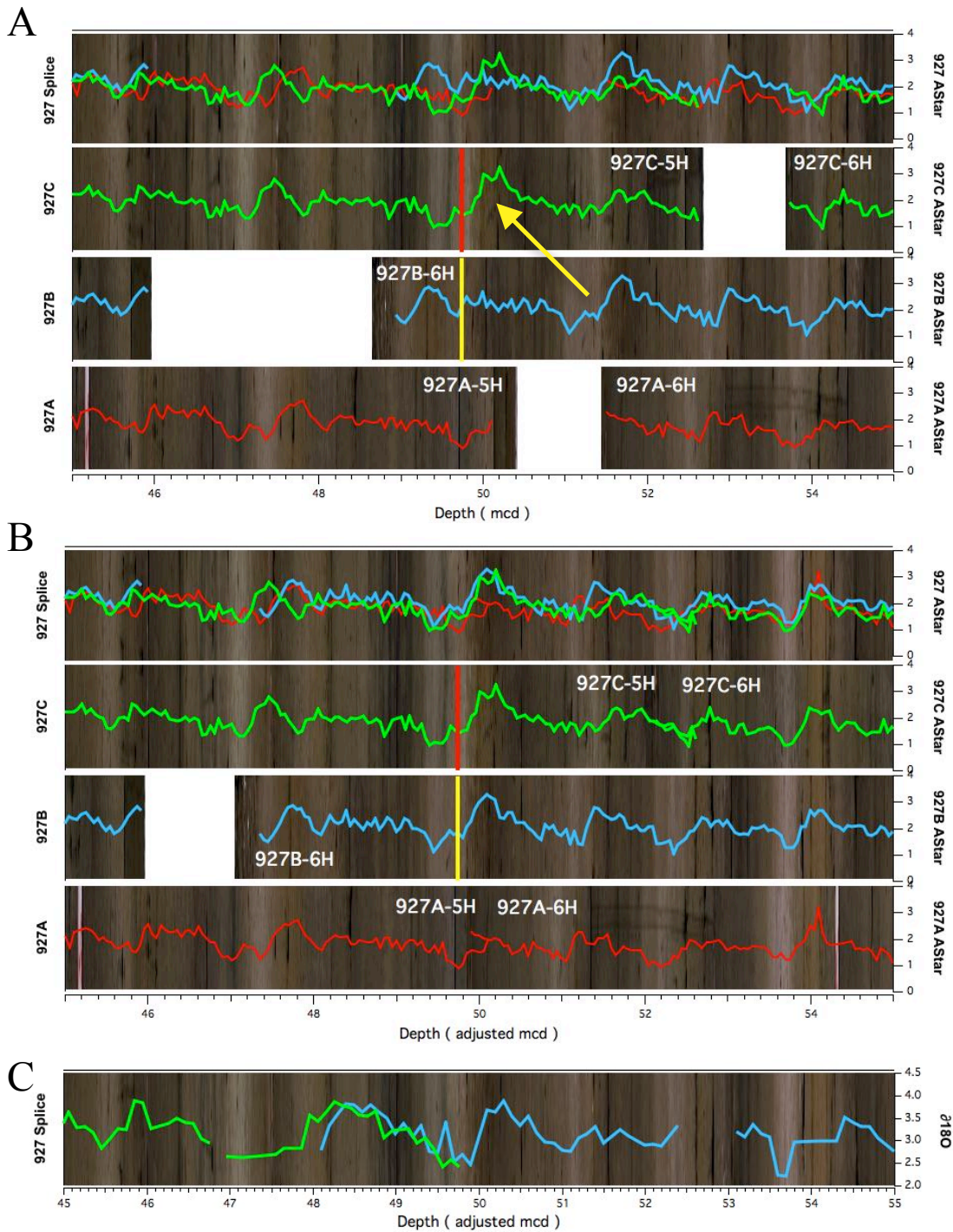
444

445 **Figure 1: The location of ODP Leg 154 Sites.**

446



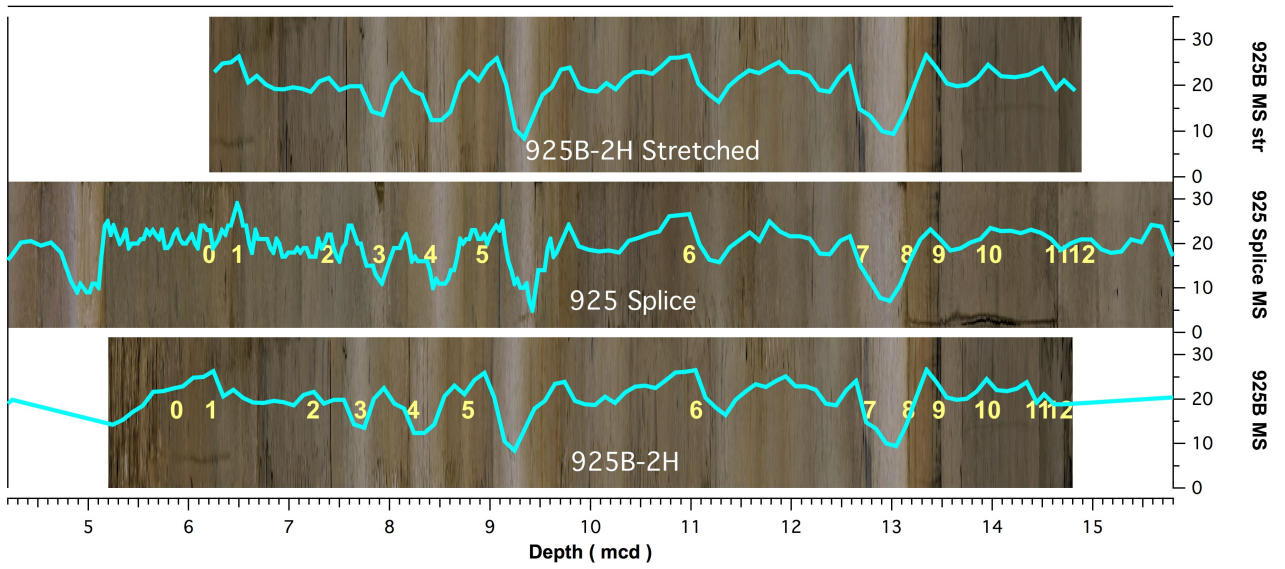
447
 448 Figure 2: Creating a composite core image from a core table image. (A) Image loaded into IGOR. Red cursor moves horizontally
 449 to set bottom locations in pixels of each section. Yellow cursor moves horizontally and vertically to the lower left corner of each
 450 section before cutting. Inset - Lengthwise lightness profiles for each of the cut sections and a best fit line used for the lighting
 451 correction. (B) Composite core image scaled to mbsf. Vertical red lines indicate section breaks. Lower image has been corrected
 452 for uneven lighting in the core box photo.



453

454

455 **Figure 3: A. Reflectance spectrophotometer (RSC) a^* data (LAB color model) and core images plotted against the**
 456 **published splice mcd. The yellow arrow indicates misaligned features. The yellow vertical line represents the top of a**
 457 **splice section and the vertical red line shows the bottom of the previous splice section. B. The revised splice. The splice**
 458 **goes from Core 927C-05H to Core 927B-06H in both cases, but the offset for Core 927B-06H has been reduced by 1.6 m in**
 459 **the revised splice to account for the repeat sampling of a cycle. Note the poor agreement of the data between 49 and 51**
 460 **mbsf in the original splice. C. Benthic $\delta^{18}O$ revised. Samples were collected based on the original splice, resulting in data**
 461 **duplication between 48 and 50 m adjusted mcd.**



462

463

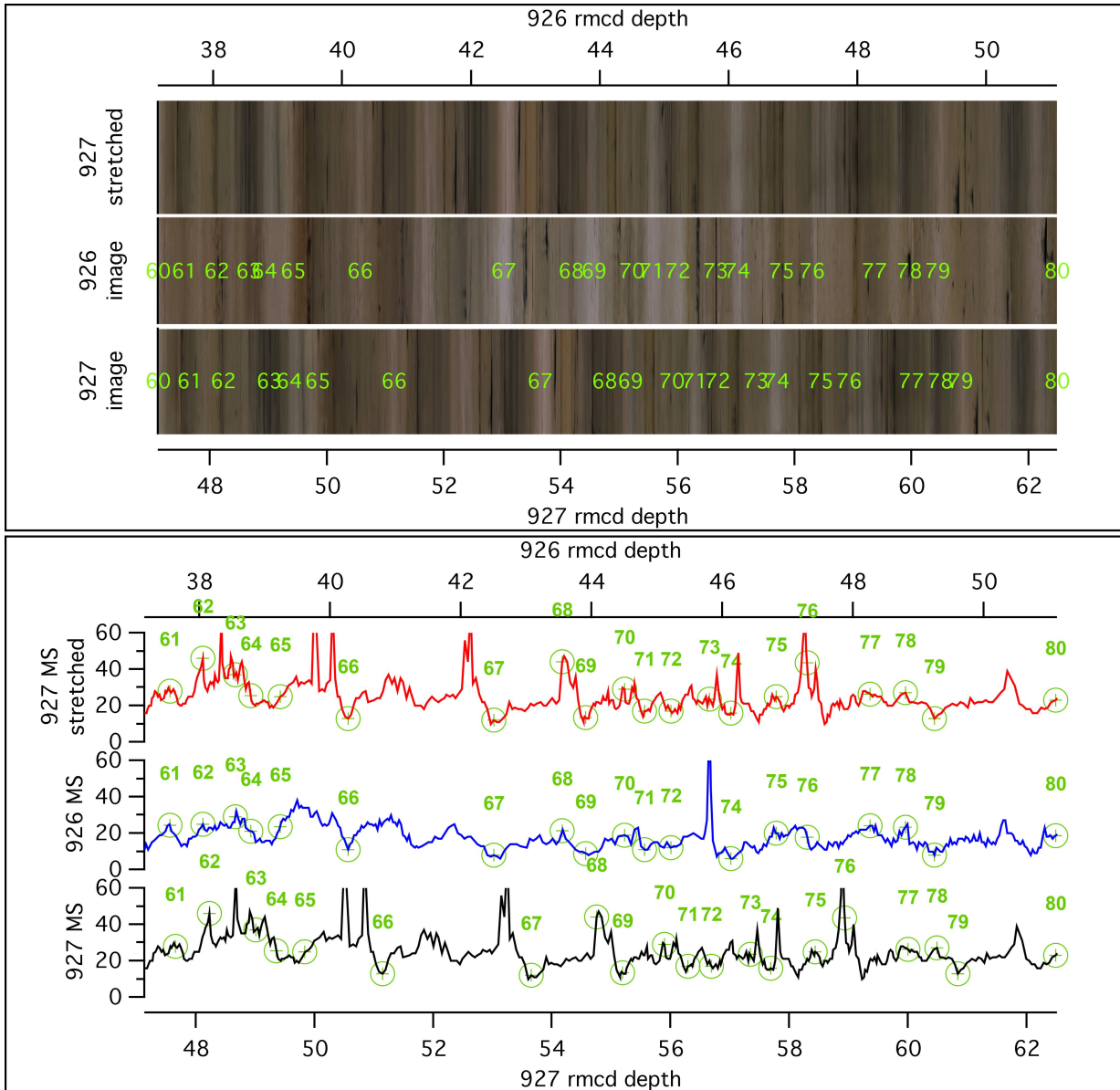
464 **Figure 4: Core 925B-2H was not used for the Site 925 splice and while there is good alignment between the core image**
 465 **and data and the spliced image and data at 13-14 mcd, shallower portions of the core are not well aligned with the splice.**

466 **Yellow numbers indicate tie points used to stretch the image and data so that they are in better agreement with the splice.**

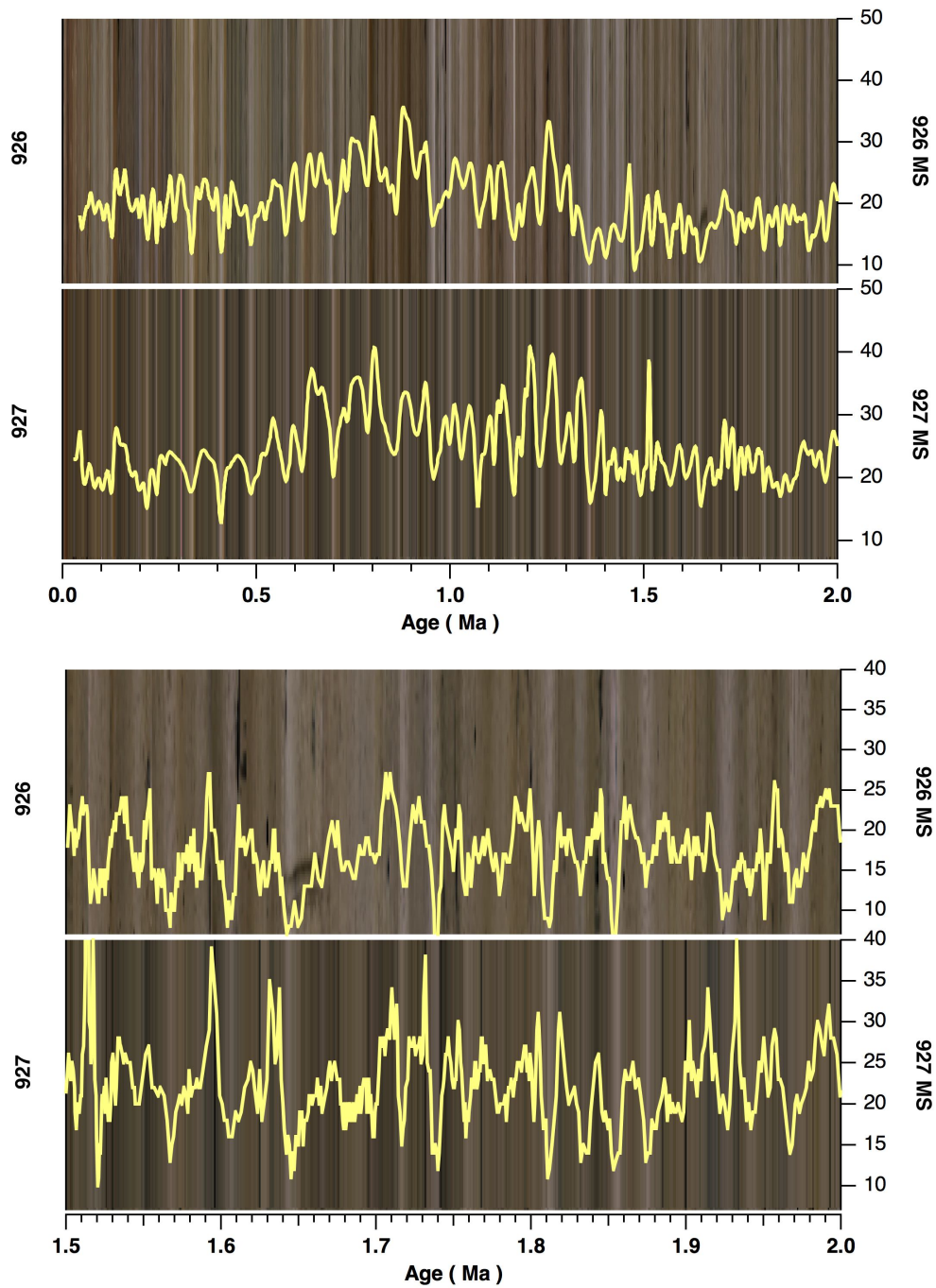
467 **Choice of tie points is cursor driven and stretching can be recalculated in real time.**

468

469



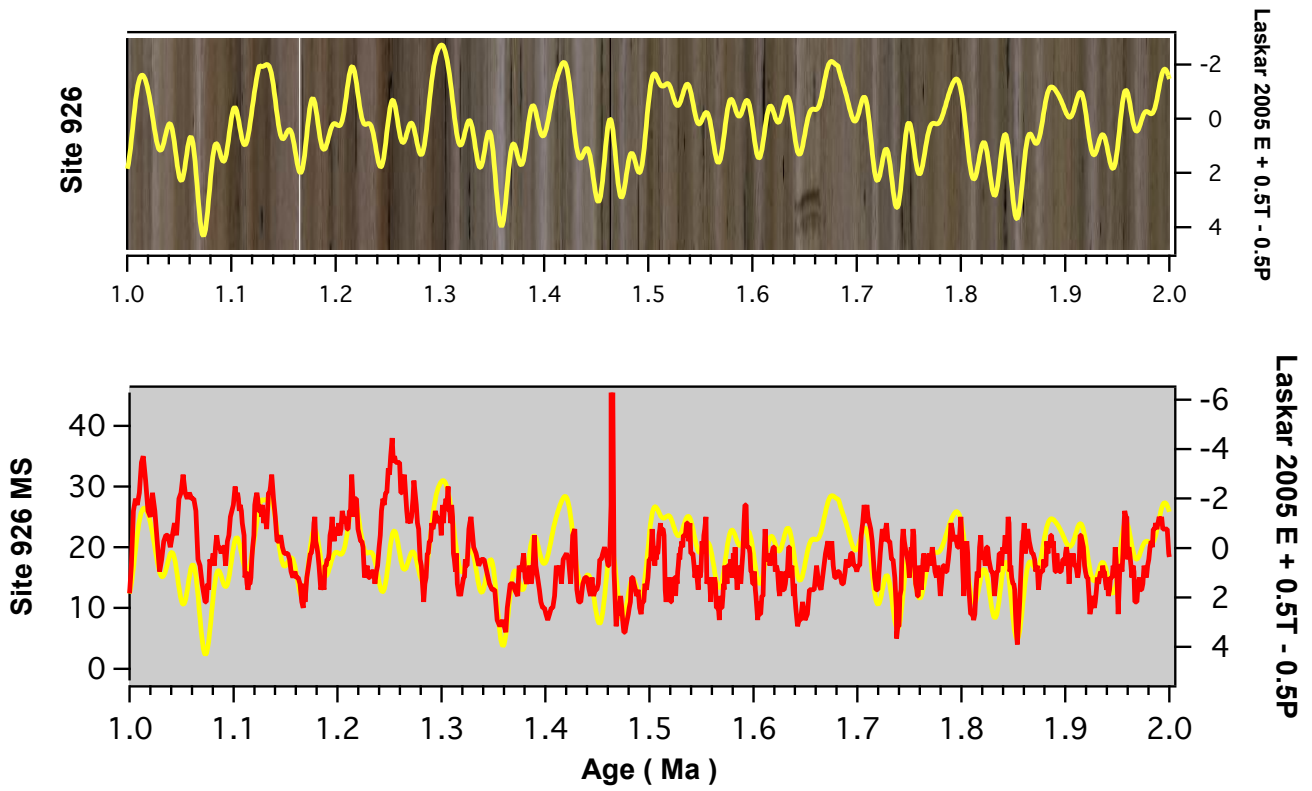
470
 471 **Figure 5: Spliced images and MS data from ODP Sites 926 and 927. The rmcd depth scales indicate that there have been**
 472 **small adjustments to the published splices for each site. Site 927 data and image are plotted versus the Site 927 depth scale**
 473 **on the bottom of each graph and versus the Site 926 depth scale at the top. Green numbers indicate tie points between the**
 474 **sites used to stretch the Site 927 image and data.**
 475



476

477 **Figure 6: Top - Smoothed MS data and images plotted versus age from 0 - 2 Ma. Bottom - 1.5 - 2 Ma detail using non-**

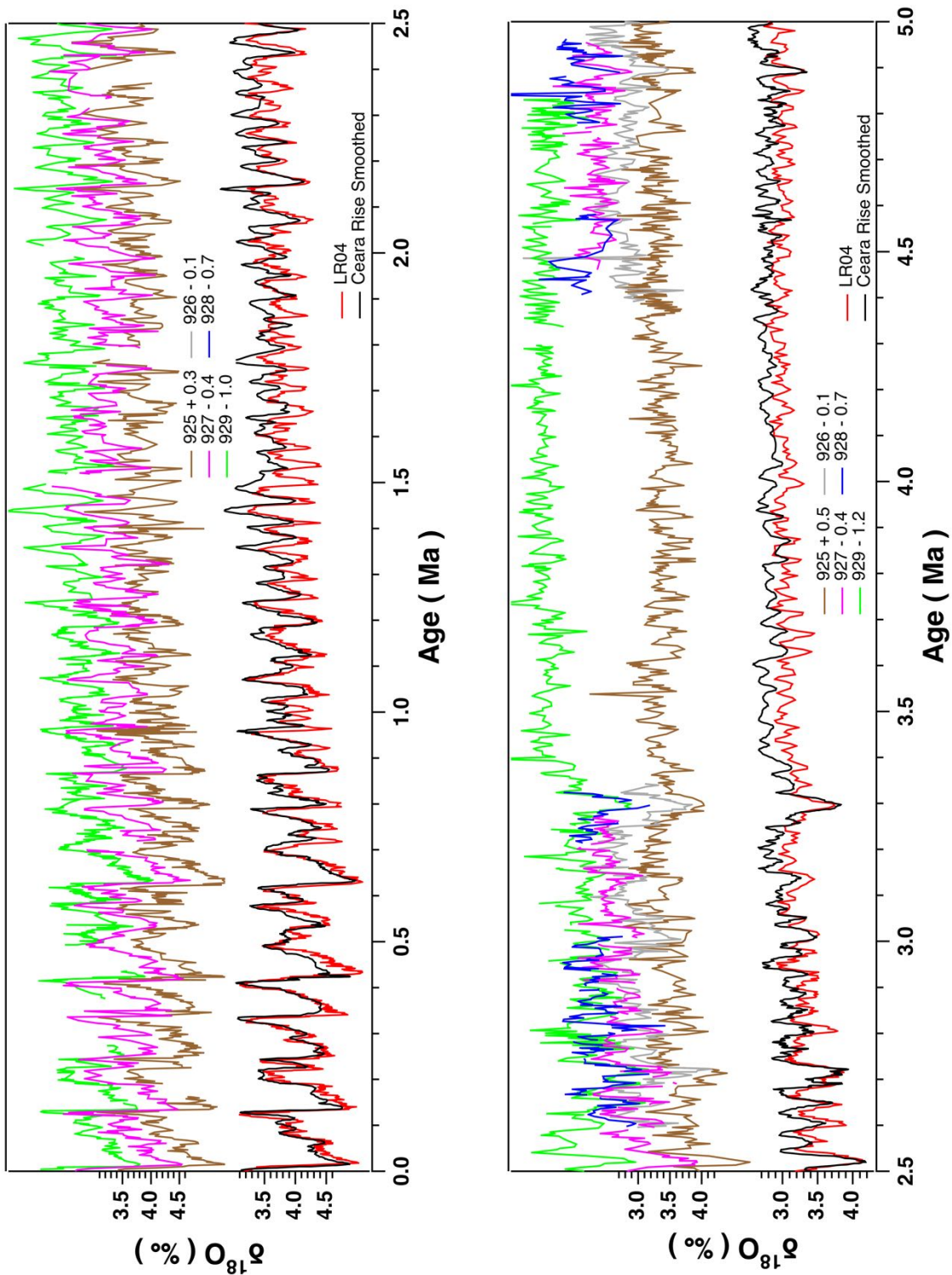
478 **smoothed data. Fine layers, on the order of 10 kyr, are correlated between Sites 927 and 926.**



479

480 **Figure 7: Laskar et al. (2004) orbital calculation compared to the Site 926 composite image and MS data. E = eccentricity,**
 481 **T = tilt (obliquity), and P = precession. The Laskar curve was compared to MS to check the age model used in this study**
 482 **that was based on the images and color reflectance. The composite image is the result of comparing multiple data sets and**
 483 **individual core images.**

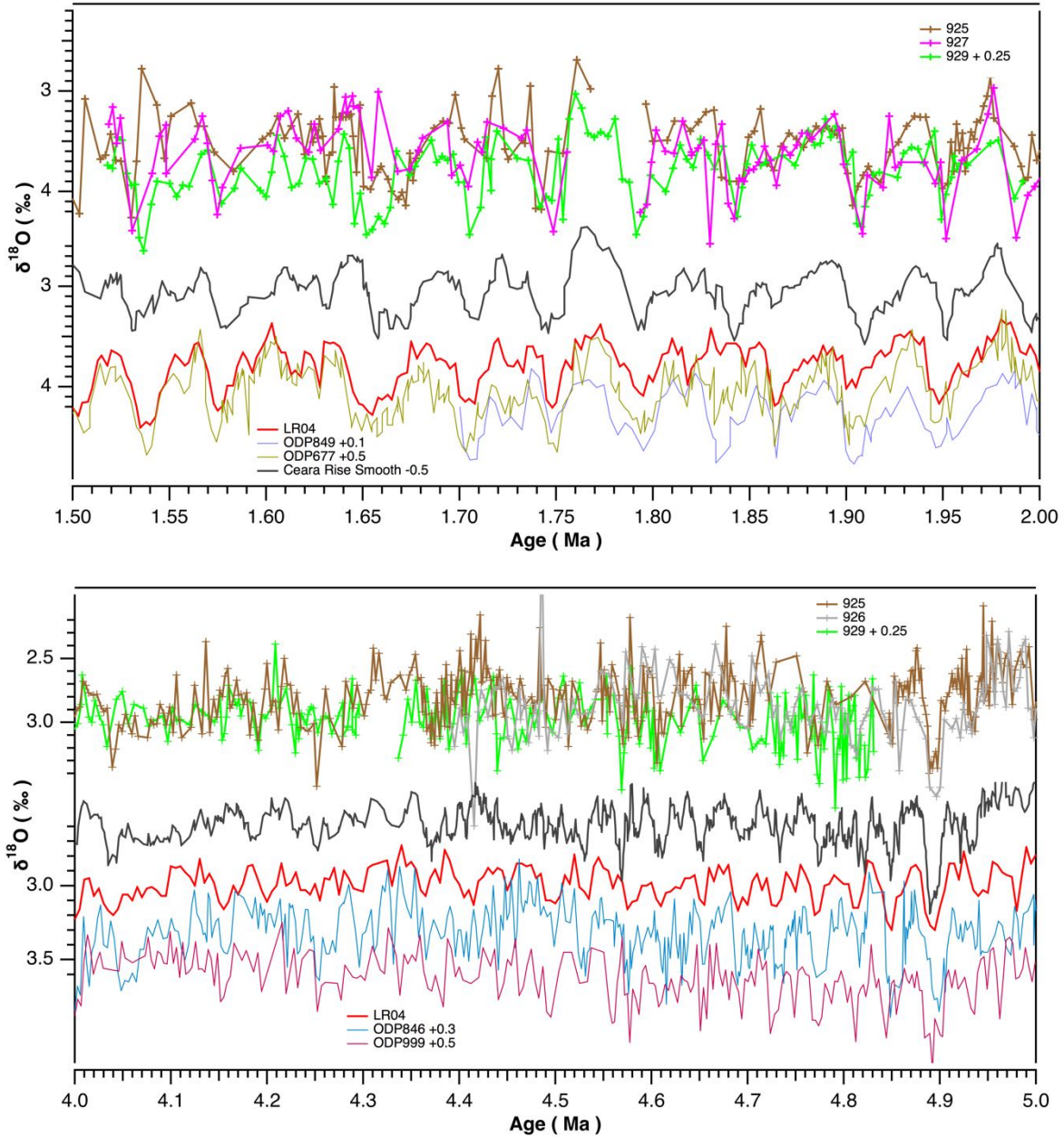
484



485
 486 Figure 8: Benthic oxygen isotope data from all Ceara Rise sites compared with one another and a smoothed composite of
 487 all data compared to LR04. Top - 0 to 2.5 Ma, bottom 2.5 to 5 Ma. Note the $\delta^{18}\text{O}$ scale change between top and bottom
 488 plots. Individual site traces have been offset as indicated in the legend.

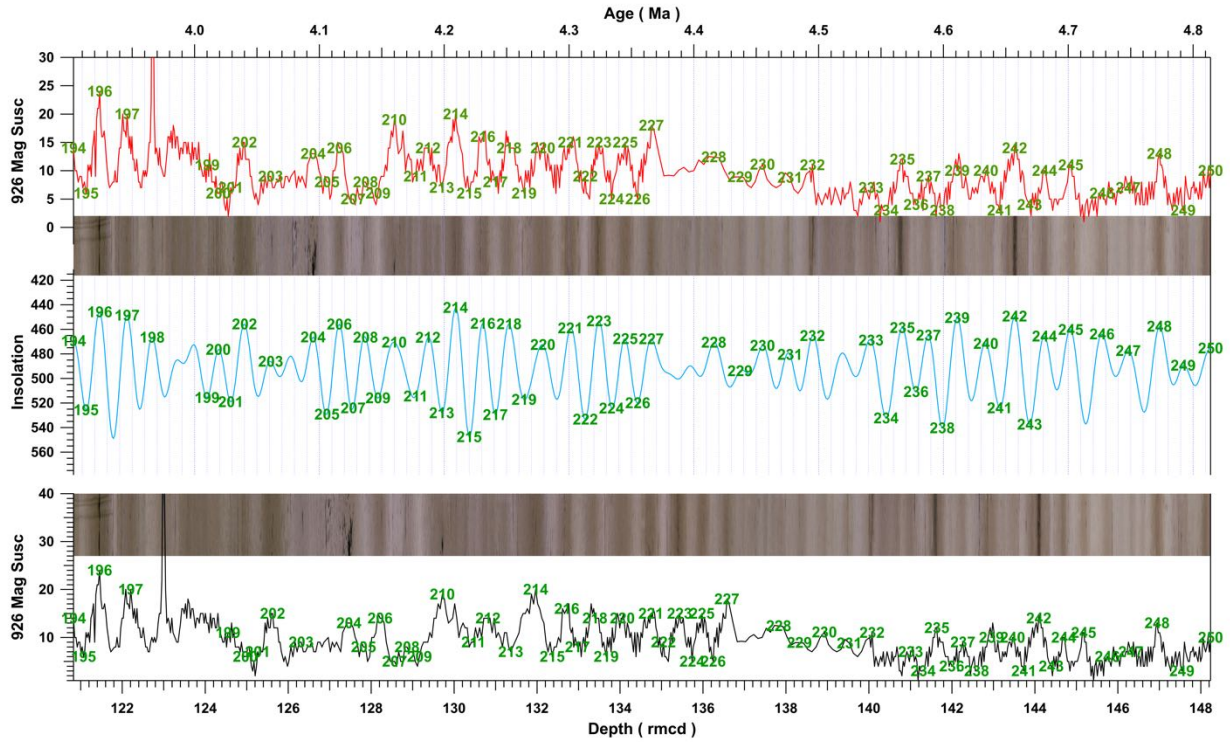
489 Original Figure 9 was removed.

490

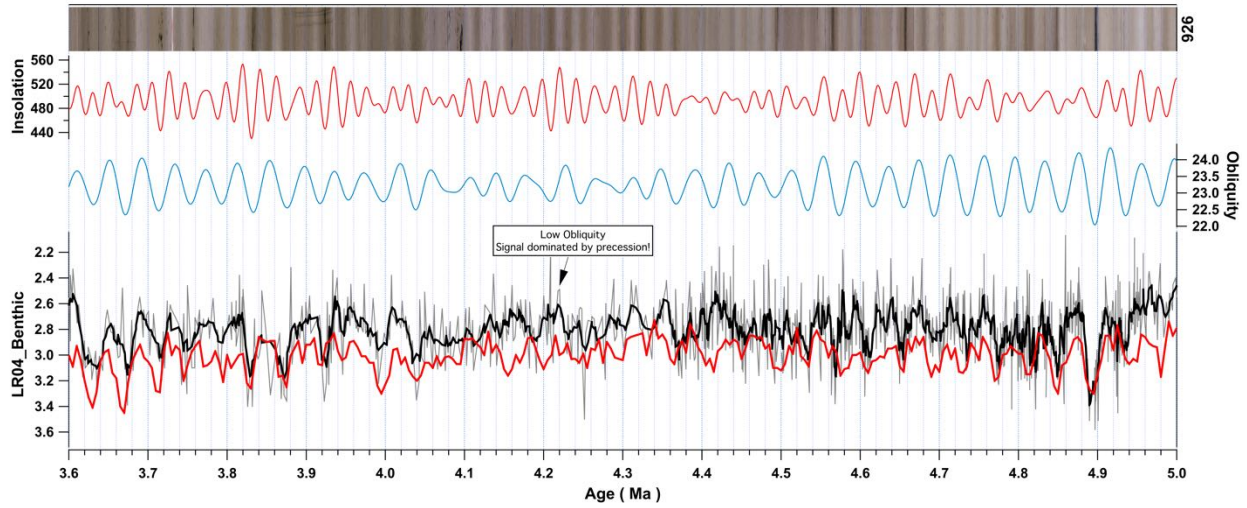


491
 492 **Figure 9: Detail from Fig. 8 comparing individual holes to one another and a smoothed composite to LR04 for the**
 493 **intervals 1.5 to 2.0 Ma and 4.0 to 5.0 Ma. For better illustration we plotted the initial alignment target records of the**
 494 **LR04 stack. For the 1.5 to 2.0 Ma interval these are the records from ODP Sites 677 and 849, for the interval 4.0 to 5.0**
 495 **Ma these are the records from ODP Sites 846 and 999. Some records have been shifted as indicated in the figure for better**
 496 **comparison of the data with each other. Note the differences between LR04 and the Ceara Rise average at 1.80 - 1.85 Ma**
 497 **although the initial alignment targets are more similar to the Ceara Rise smooth. Also note the difference between 4.0 and**
 498 **4.5 Ma. The Site 999 record is from a single hole and the splice of the Site 846 record might be erroneous. The age model**
 499 **for the Ceara Rise is very robust in this interval (see. Fig. 10) pointing to potential inconsistencies in the age model**
 500 **construction of the Site 846 and Site 999 records.**

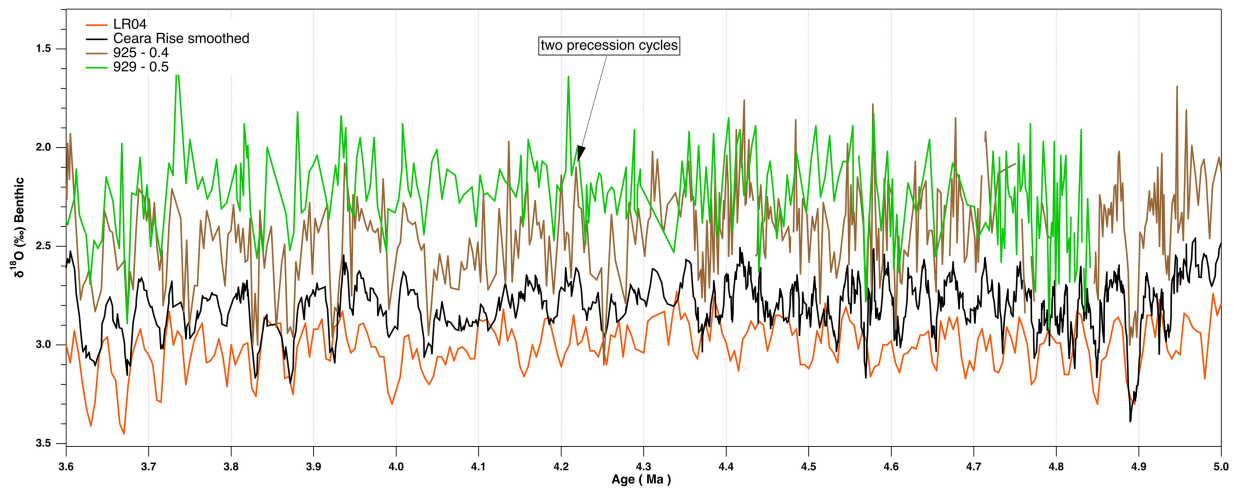
501



502
 503 **Figure 10: Detail from CODD tuning of Site 926 magnetic susceptibility and core images to insolation.**
 504 **Bottom is data versus depth, middle shows insolation 65°N 21st June inverted, and top shows image and**
 505 **magnetic susceptibility versus tuned age. Green numbers mark position of tie points. Numbers identify tie**
 506 **points between the data and the insolation curve. Light/dark layering in the composite core image is tied to**
 507 **precession cycles prominent in the insolation curve.**
 508



509
 510 **Figure 11: A comparison of LR04 (Red) to Ceara Rise (grey and black (smooth)) to obliquity and insolation from Laskar**
 511 **et al. 2004. Note that the interval 4.0 and 4.5 Ma exhibits poorly defined obliquity cycles leaving insolation dominated by**
 512 **precession.**



513
 514
 515 **Figure 12: A comparison of LR04 and Ceara Rise (smooth) to Site 925 and Site 929 benthic isotope data. LR04**
 516 **assignment of variability in the interval from 4.0 to 4.5 Ma to precession peaks may have resulted in the mismatch with**
 517 **the Ceara Rise stack.**

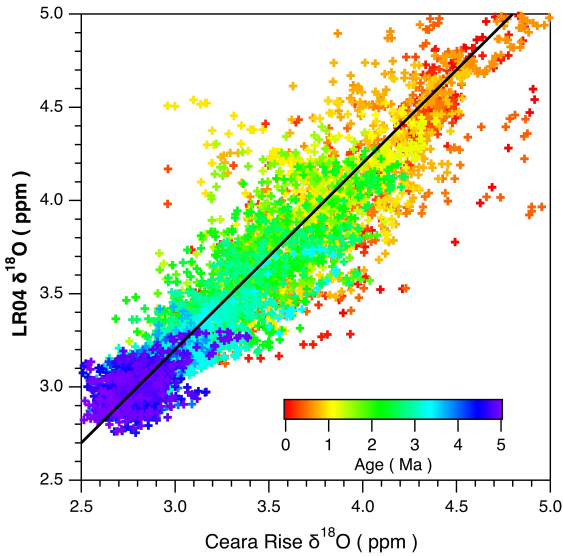


Figure S1: A comparison between the oxygen isotope data from the smoothed Ceara Rise composite and the LR04 global compilation. The black line represents a 1:1 correspondence that has been shifted by +0.2 ppm along the LR04 axis.

529

530 IGOR CODD Functions, a User Guide, and Help files may be downloaded at www.CODD-Home.net.

531

532 Data Tables may be found on the PANGAEA database at <https://doi.pangaea.de/10.1594/PANGAEA.870873>.

533 The tables include:

534 For each site

535 Offset table

536 Splice interval table

537 Spliced magnetic susceptibility (MS) data including Site 926 equivalent depths

538 Isotope data including Site 926 equivalent depths

539 Age model including Site 926 equivalent depths

540 Stretching tie points for each hole (offsplice depths vs splice depths)

541 Table of species abbreviations for isotope tables

542 Leg 154 Combined benthic isotope data

543 Leg 154 Smoothed benthic isotope data

544 Site to site tie tables linking sites 925, 927, 928, and 929 to site 926

545 Core images (lighting corrected) for all Leg 154 cores in png format with depth scale and as depth scaled

546 Igor binary files